Contribution from the Department of Chemistry,
Boston College, Chestnut Hill, Massachusetts 02167

Electron-Transfer Properties of Potassium Tetrachloroaurate(III), Gold(I) Trialkylphosphine, and Gold(I) Trialkyl Phosphite Complexes in Nonaqueous Media

J. E. Anderson,* S. M. Sawtelle, and C. E. McAndrews

Received August 1, 1989

An electrochemical and spectroelectrochemical investigation of $Au[P(R)_3]Cl$, where R = C_2H_5, C_6H_5, OC_2H_5, and OC_6H_5, and $Au[P(R)_3]_2Cl$, where R = C_6H_5 and OC_2H_5, in acetonitrile (CH_3CN), tetrahydrofuran (THF), or dichloromethane (CH_2Cl_2) with tetrabutylammonium perchlorate (TBAP) as supporting electrolyte is presented. The experiments were performed in the absence of both water and oxygen, and under these conditions, the gold(I) complexes are oxidized by a ECE(C) process to generate $[AuX_4]^-$, X = Cl^- and ClO_4^-. Reduction of $[AuX_4]^-$ in the presence of $P(R)_3$ results in regeneration of $Au[P(R)_3]Cl$. The potential for the oxidation of $Au[P(R)_3]Cl$ and $Au[P(R)_3]_2^+$ is dependent upon the nature of the ligands and the solvent conditions. Electrochemical data for $K[AuCl_4]$ are also presented and are consistent with an electron-transfer mechanism previously proposed for the reduction of $H[AuCl_4]$. By the use of electrochemical, spectroelectrochemical, and conductivity data, an electron-transfer mechanism for the gold species is presented.

(Triethylphosphine)gold(I) chloride, $Au[P(C_2H_5)_3]Cl$, is one of several gold(I) complexes that exhibit activity against rheumatoid arthritis.[1-3] Attempts to understand the function of this complex have led to numerous investigations of the chemical and biochemical properties of the compounds $Au[P(R)_3]Cl$ and $Au[P(R)_3]_2Cl$.[4-10] Upon introduction into models of biological systems, these complexes undergo ligand exchange. Chemical redox reactions are also observed and are proposed to occur following loss of $P(R)_3$ from $Au[P(R)_3]Cl$ or $Au[P(R)_3]_2Cl$.[7-9,11]

While the ligand-exchange reactions of $Au[P(R)_3]Cl$ and $Au[P(R)_3]_2Cl$ have been investigated,[4,12-14] their electron-transfer properties are not known. This includes oxidation potentials, how ligand substitution changes these values, and what intermediates and final products are formed upon electron transfer. The effects of different solvent conditions on the electron-transfer mechanism are also unknown.

In this paper, we will present an electrochemical and spectroelectrochemical investigation on $Au[P(R)_3]Cl$, where R = C_2H_5, C_6H_5, OC_2H_5, and OC_6H_5 and $Au[P(R)_3]_2Cl$, where R = C_6H_5 and OC_2H_5. Data for $K[AuCl_4]$ will also be presented. The experiments were performed under an inert atmosphere, and the solvent system was either acetonitrile (CH_3CN), tetrahydrofuran (THF), or dichloromethane (CH_2Cl_2) with tetrabutylammonium perchlorate (TBAP) as supporting electrolyte.

Under these conditions, the gold(I) complexes are oxidized by a ECE(C) electron-transfer process to generate a gold(III) species, formulated as $[AuX_4]^-$, X = Cl^- and ClO_4^-, on the basis of electrochemical and spectroscopic data. $Au[P(R)_3]Cl$ is formed upon rereduction of the electrogenerated $[AuX_4]^-$. The potential for the oxidation of $Au[P(R)_3]Cl$ and $Au[P(R)_3]_2^+$ is dependent upon the nature of the ligands and the solvent conditions.

The electrochemical data for $K[AuCl_4]$ are consistent with the electron-transfer mechanism previously proposed for the reduction of $H[AuCl_4]$.[15] The addition of $P(R)_3$ to solutions of $K[AuCl_4]$ to generate either $Au[P(R)_3]Cl$ or $Au[P(R)_3]_2Cl$ was monitored electrochemically, and in some cases the reaction was electrochemically driven. From the electrochemical, spectroelectrochemical, and conductivity data, a self-consistent electron-transfer mechanism for these gold species will be presented.

In general, there are very little electrochemical data on gold complexes that have biological significance.[16] The standard potentials for the metallic gold/$Au(L)_2$, L = thiosulfate, cysteine, thiocyanate, and bromide, couples have been published.[17-21] Aqueous potentiometric titration data with a mercury electrode for some of the gold(I) drugs have been previously reported.[22] Our data are not directly comparable to the previous studies due to different solvent systems and measurement of different electron-transfer reactions. However, the data in this paper and that previously reported suggest electrochemistry may provide insight into the function of gold(I) drugs.[22]

Experimental Section

Materials. All reagents for synthesis were purchased at the highest level of purity available and were used without further purification. For electroanalysis, spectroscopic grade acetonitrile, tetrahydrofuran, and dichloromethane were purchased (Aldrich), purified by standard techniques,[23,24] stored over calcium hydride (CH_3CN), phosphorus pentoxide (CH_2Cl_2), or sodium/benzophenone (THF) under an inert atmosphere, and distilled just prior to use. Tetrabutylammonium perchlorate (TBAP) was purchased from Fluka, twice recrystallized from ethanol, and dried in a vacuum oven at 50 °C.

Gold Complexes. $K[AuCl_4]$ was purchased from AESAR, $Au[P(C_2H_5)_3]Cl$ was purchased from Aldrich, and both were used without further purification. $Au[P(C_6H_5)_3]Cl$ was synthesized by published methods[4,25,26] and characterized by comparison with published spectra.

(1) *Primer to the Rheumatic Diseases*, 7th ed.; Rodnan, G. P., Ed.; The Arthritis Foundation, American Medical Association: New York, 1973.
(2) Sutton, B. M. *Platinum, Gold, and Other Metal Chemotherapeutic Agents*; Lippard, S. J., Ed.; ACS Symposium Series 209; American Chemical Society: Washington, DC, 1983; p 355.
(3) Sadler, P. J. *Struct. Bonding* **1976**, *29*, 171.
(4) Puddephatt, R. J. In *Comprehensive Coordination Chemistry*; Wilkinson, G., Ed.; Pergamon Press: New York, 1987; Vol. 5, p 861.
(5) Brown, D. H.; Smith, W. C. *Chem. Soc. Rev.* **1980**, *9*, 217.
(6) Melnik, M.; Parish, R. V. *Coord. Chem. Rev.* **1986**, *70*, 157.
(7) Isab, A. A.; Hormann, A. L.; Hill, D. T.; Griswold, D. E.; DiMartino, M. J.; Shaw, C. F. *Inorg. Chem.* **1989**, *28*, 1321.
(8) Razi, M. T.; Otiko, G.; Sadler, P. J. *Platinum, Gold, and Other Metal Chemotherapeutic Agents*; Lippard, S. J., Ed.; ACS Symposium Series 209; American Chemical Society, Washington, DC, 1983; p 371.
(9) Shaw, C. F.; Coffer, M. T.; Hormann, A. C.; Mirabelli, C. K.; Crooke, S. T. *J. Inorg. Biochem.* **1987**, *30*, 177.
(10) Berners-Price, S. J.; Sadler, P. J. *Inorg. Chem.* **1986**, *25*, 3822.
(11) Malik, N. A.; Otiko, G.; Sadler, P. J. *J. Inorg. Biochem.* **1980**, *12*, 317.
(12) Lewis, G.; Shaw, F. C. *Inorg. Chem.* **1986**, *25*, 58.
(13) Boles-Bryan, D. L.; Mikuriva, Y.; Hempel, J. C.; Mellinger, D.; Hashim, M.; Pasternack, R. F. *Inorg. Chem.* **1987**, *27*, 4180.
(14) Echer, D. J.; Hempel, J. C.; Sutton, B. M.; Kirsch, R.; Crooke, S. T. *Inorg. Chem.* **1986**, *25*, 3139.
(15) Goolsby, A.; Sawyer, D. T. *Anal. Chem.* **1968**, *13*, 1978.
(16) Schmid, G. M. In *Standard Potentials in Aqueous Solution*, 1st ed.; Bard, A. J., Parsons, R., Jordon, J., Eds.; M. Dekker: New York, 1985; p 313.
(17) Pouradier, J.; Gadet, M.-C. *J. Chim. Phys. Physiochim. Biol.* **1969**, *66*, 109.
(18) Pouradier, J.; Gadet, M.-C. *J. Chim. Phys. Physiochim. Biol.* **1965**, *62*, 1181.
(19) Chernyak, A. S.; Shertopalova, L. F. *Russ. J. Inorg. Chem.* (*Engl. Transl.*) **1976**, *21*, 464.
(20) Pouradier, J.; Gadet, M.-C. *J. Chim. Phys. Physiochim. Biol.* **1963**, *63*, 1467.
(21) Martins, M. E.; Castellano, C.; Calandra, A. J.; Arvia, A. J. *J. Electroanal. Chem. Interfacial Electrochem.* **1977**, *81*, 291.
(22) Huck, F.; Medicis, R.; Lussier, A.; Dupuis, G.; Federlin, P. *J. Rheumatol.* **1984**, *11*, 605.
(23) Gordon, A. J.; Ford, R. A. *The Chemist's Companion*; Wiley Interscience: New York, 1972; p 408.
(24) Kadish, K. M.; Anderson, J. E. *Pure Appl. Chem.* **1987**, *59*, 5, 707.

0020-1669/90/1329-2627$02.50/0

Table I. Electrochemical Data for the Studied Complexes (Scan Rate = 100 mV/s)

complex	solvent	concn, mM[a]		E_p, V vs SCE					
		Au	$P(R)_3$	1	2	3	4	5	Fc[b]
$K[AuCl_4]$	CH_3CN	4.3		0.07	−0.08				
	THF	8.8		−0.17[c]					
	CH_2Cl_2	4.6		−0.05[c]					
$Au[P(C_2H_5)_3]Cl$	CH_3CN	3.4				1.51	0.20		0.40
	THF	4.2				*d*	*d*		
	CH_2Cl_2	5.2				1.73	0.03		0.39
$Au[P(C_6H_5)_3]Cl$	CH_3CN	3.4				1.54	0.03		0.40
	CH_2Cl_2	4.4				1.67	*e*		0.45
$Au[P(OC_2H_5)_3]Cl$	CH_3CN	4.4[f]	5.8	0.00[c]		1.86			
$Au[P(OC_6H_5)_3]Cl$	CH_3CN	4.5[f]	4.6	−0.05[c]		1.76			
$Au[P(C_6H_5)_3]_2^+$	CH_3CN	4.8[g]	11.2				*e*	0.78	0.40
	CH_2Cl_2	4.4[g]	23.7				*e*	1.00	0.43
$Au[P(OC_2H_5)_3]_2^+$	CH_3CN	4.4[f]	35.0					1.10	0.40

[a] Concentration of the gold complex and/or the added $P(R)_3$ ligand in the cyclic voltammetric experiment. [b] $E_{1/2}$ for the ferrocene/ferrocenium couple as internal standard. [c] Process 1 and 2 are merged under these conditions. See text. [d] Wave not observed under these conditions. See text. [e] More negative than −0.10 V; for example, see Figure 6b. [f] Concentration of $K[AuCl_4]$ at start of experiment. [g] Concentration of $Au[P(C_6H_5)_3]Cl$ at start of experiment.

Elemental analysis was obtained for $Au[P(C_6H_5)_3]Cl$ and gave the following results. Calcd: C, 43.67; H, 3.05. Found: C, 44.50; H, 3.04.

The complexes $Au[P(R)_3]Cl$, R = OC_2H_5 and OC_6H_5, and $Au[P(R)_3]_2Cl$, R = C_6H_5 and OC_2H_5, were synthesized and examined in situ and were characterized by UV–visible,[25,26] conductivity,[27] and electrochemical data.

Equipment and Techniques. Electrochemical experiments were performed with either a BAS-100A or a EG&G Princeton Applied Research 273 potentiostat/galvanostat coupled to an EG&G Princeton Applied Research Model RE0091-XY recorder. A platinum-button working electrode, approximate area 0.008 cm^2, a platinum-wire counter electrode, and an SCE reference electrode, separated from the solution with a bridge, comprised the three-electrode system. All potentials were measured vs a SCE reference electrode, and the ferrocene/ferrocenium couple was also used as an internal standard. The supporting electrolyte was 0.1 M TBAP, unless otherwise stated. Low-temperature data were recorded by cooling the cell with a dry ice/acetone bath, monitored with a thermometer. Spectroelectrochemical data were recorded on a Perkin-Elmer Lambda 3B UV–vis spectrophotometer using an BAS CV-27 potentiostat coupled to an IBM 7424 MT X-Y-T recorder. In this case, the electrodes used were a large platinum working minigrid electrode, a platinum-wire counter electrode, and either an Ag/AgCl reference electrode separated from the solution with a bridge or a wire pseudoreference electrode. The supporting electrolyte was 0.2 M TBAP, unless otherwise stated. The electrochemical cells are homebuilt and are designed for inert-atmosphere studies. UV–visible spectra were recorded on a Perkin-Elmer Lambda 3B instrument, and conductivity experiments were performed on a YSI Model 31A conductivity bridge.

Abbreviations used in this text follow standard electrochemical convention.[29] For example, E_p is peak potential, v is scan rate, and i_p is peak current.

Results and Discussion

$K[AuCl_4]$. Figure 1 is the cyclic voltammogram obtained at 100 mV/s for a 0.0043 M solution of $K[AuCl_4]$ in 0.40 M TBAP, CH_3CN. When the potential is scanned from 0.3 to −0.5 V, two overlapping reduction processes at E_{pc} = 0.07 and −0.08 V vs SCE (waves 1 and 2, Figure 1a) are observed. No oxidation waves are found upon scanning from 0.3 V to 2.0 V, but after scanning negative of wave 1 and 2, a small oxidation processes is observed at E_{pa} = 1.26 V vs SCE (wave 1.1, Figure 1b). Wave 1.1 may be a combination of two waves, but the current is too low for an accurate characterization. A reduction process is also coupled with wave 1.1, as shown in Figure 1b. Waves 1 and 2 are not resolved in either THF or CH_2Cl_2, and under these conditions a broad combination wave is found. The potentials for reduction of $K[AuCl_4]$ in these three solvent systems are in Table I.

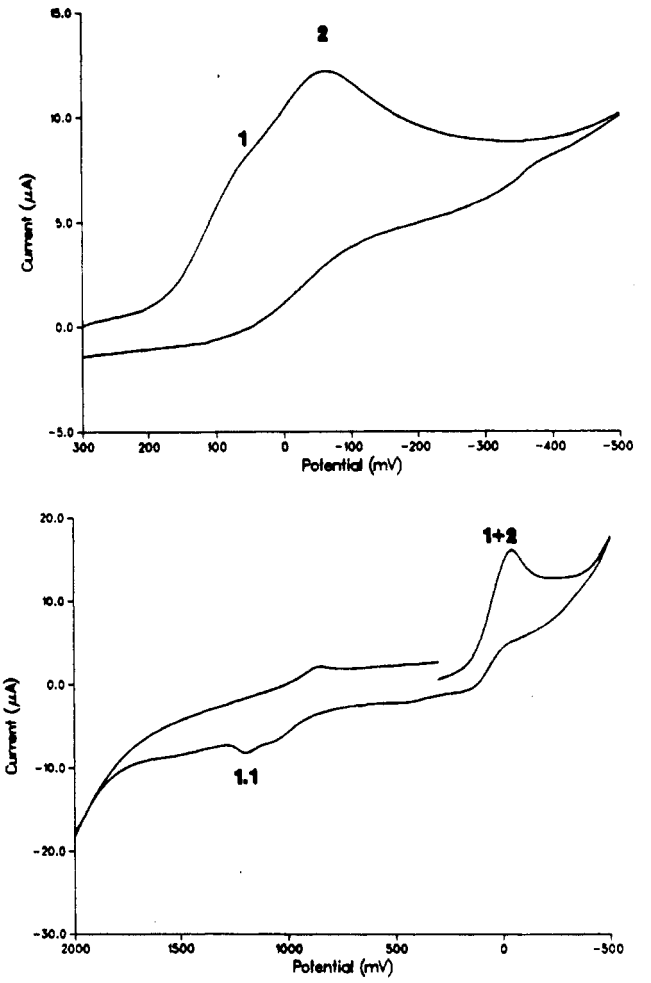

Figure 1. Cyclic voltammograms of a 0.0043 M solution of $K[AuCl_4]$ in acetonitrile, 0.400 M TBAP at 100 mV/s: (a, top) potential scan from 300 to −500 mV; (b, bottom) potential scan from 300 to −500 to 2000 mV.

The reduction of $K[AuCl_4]$ is an irreversible electron-transfer processes in the sense that there are no oxidation waves coupled to waves 1 and 2 up to scan rates of 1000 mV/s. Oxidation processes associated with this reduction are also not observed at low temperature, but under these conditions (−30 °C, acetonitrile) waves 1 and 2 are merged into one process in the cyclic voltammogram. Waves 1 and 2 shift in a negative direction with increasing scan rate, and these data are consistent with relatively fast chemical reactions associated with electron transfer.[28-30]

(25) Mann, F. G.; Wells, A. F.; Purdie, D. *J. Chem. Soc.* **1937**, 1828.
(26) Roulet, R.; Lan, N. Q.; Mason, W. R.; Fenske, G. P. *Helv. Chim. Acta* **1973**, *56*, 2405.
(27) Westland, A. D. *Can. J. Chem.* **1969**, *47*, 4135.
(28) *Electrochemical Methods*; Bard, A. J., Faulkner, L. R., Eds.; John Wiley & Sons: New York, 1980. See pages vii–xvi for a list of abbreviations.
(29) Nicholson, R. S.; Shain, I. *Anal. Chem.* **1965**, *37*, 178.

The value of $E_{pc} - E_{pc/2}$ is 39 mV for wave 1 and 82 mV for wave 2 in Figure 1a, but these values are difficult to obtain due to the overlap of the waves and may not be accurate. The ratio of the peak current to the square root of scan rate ($i_p/v^{1/2}$) is constant for both waves and implies diffusion-controlled processes.

Two reduction waves at $E_{1/4}$ of 0.08 and −0.41 V vs SCE were reported in an chronopotentiometry study of $H[AuCl_4]$ in acetonitrile.[15] The process at −0.41 V was assigned to the reduction of H^+, while the process at 0.08 V was assigned as an three-electron reduction of $[AuCl_4]^-$ to form metallic Au and Cl^- by the mechanism shown in eqs 1–3.[15] The intermediate $[AuCl_2]^+$ is probably solvated and of the form $[AuCl_2S_2]^+$, where S is solvent.

$$[AuCl_4]^- \rightleftharpoons [AuCl_2]^+ + 2Cl^- \quad (1)$$

$$[AuCl_2]^+ + 2e^- \rightleftharpoons [AuCl_2]^- \quad (2)$$

$$[AuCl_2]^- + e^- \rightleftharpoons Au + 2Cl^- \quad (3)$$

In agreement, bulk electrolysis of $K[AuCl_4]$ in acetonitrile at −0.20 V vs SCE results in formation of a gold film on the electrode and gives values of n of 3.5 ± 0.5. Hence, our electrochemical data are consistent with two electron-transfer steps and a total of three electrons for the reduction of $[AuCl_4]^-$ to form metallic gold. On the basis of the proposed mechanism, wave 1 and 2 in Figure 1 would be assigned to eqs 2 and 3 for the reduction of $K[AuCl_4]$. However, it should be noted that the dependence of wave 1 and 2 on scan rate and the value of $E_{pc} - E_{pc/2}$ for wave 1 and 2 neither support nor disprove the exact steps of the mechanism given in eqs 1–3.[28-30]

Wave 1.1 is due to oxidation of either the Au film or free chloride ion, both of which are generated by the reduction of $K[AuCl_4]$. Under our conditions, chloride ion is oxidized at E_{pa} = 1.05 V with a coupled reduction process at E_{pc} = 0.75 V vs SCE at 100 mV/s, which is in agreement with literature values.[31] On the basis of previous studies,[15,16] the gold film is oxidized at potentials near process 1.1 and results in generation of Au(I) species in solution. However, the oxidation potential for the gold film is very sensitive to the solvent conditions, particularly the chloride ion concentration. It is also possible that wave 1.1 is due to both processes.

Spectroelectrochemical results on $K[AuCl_4]$ are in general agreement with the mechanism given in eqs 1–3. This is shown in Figure 2, which shows the spectroelectrochemical data obtained from a 0.0049 M solution of $K[AuCl_4]$ in CH_3CN, TBAP. $K[AuCl_4]$ is characterized by absorption bands at 321 and 225 nm. Note that at this concentration, the absorption band at 225 nm is off scale. As shown in Figure 2 both absorption bands decrease to the baseline upon reduction at potentials negative of wave 1 and 2. However, no new absorption bands appear between 850 to 200 nm, which supports the loss of Au species in solution upon reduction.

If the potential at the electrode is set negative of wave 1.1 following reduction, no spectral changes are observed. However, if the potential is set positive of wave 1.1, regeneration of $[AuCl_4]^-$ is found. This suggests that wave 1.1 is due, in part, to reoxidation of the gold film on the electrode generated upon reduction of $[AuCl_4]^-$.

Parts a and b of Figure 3 show the cyclic voltammograms obtained upon the addition of either triphenylphosphine (Figure 3a) or triphenyl phosphite (Figure 3b) to solutions of $K[AuCl_4]$ in acetonitrile, TBAP. In both cases, the concentration ratio of $P(R)_3$ to Au is approximately 1:1.

Significant changes are found in the electrochemistry of $K[AuCl_4]$ upon addition of triphenylphosphine, as shown in Figure 3a. Wave 2 shifts to E_{pc} = −0.23 V, while wave 1 is at E_{pc} = 0.02 V vs SCE at 100 mV/s. In addition, a large broad oxidation wave at E_{pa} = 1.45 V vs SCE at 100 mV/s (wave 3, Figure 3a) is

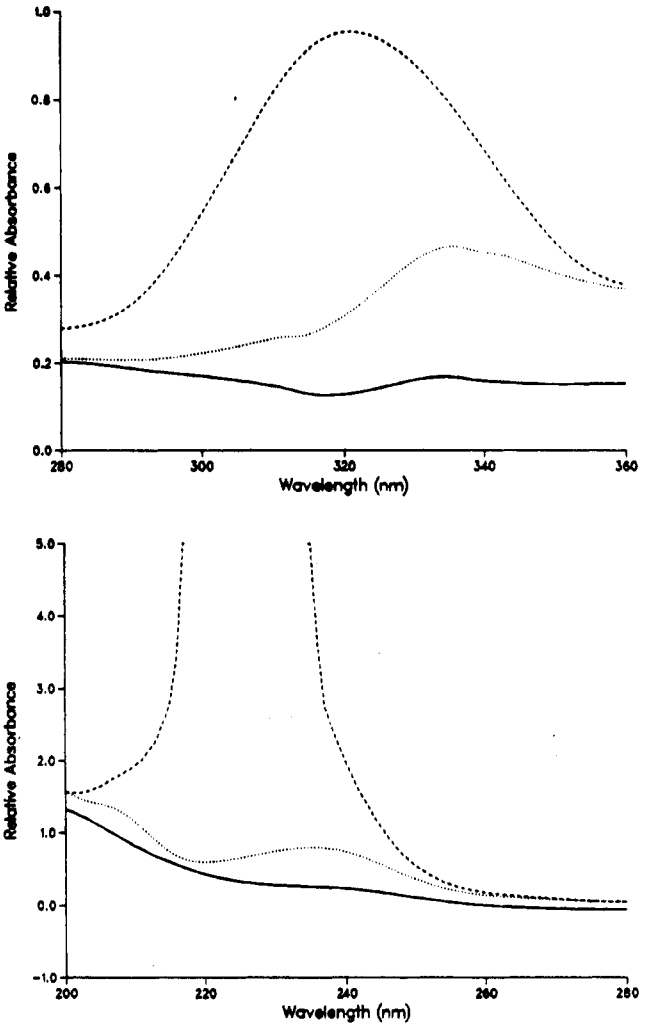

Figure 2. Spectroelectrochemical data for a 0.0049 M solution of $K[AuCl_4]$ in acetonitrile, 0.20 M TBAP: (a, top) spectral range 280–360 nm, E = −0.70 V; (b, bottom) spectral range 200–280 nm, E = −0.70 V. Key: original complex (- - -); T = 20 s (···); T = 2 min (—). Potentials are vs a Pt wire pseudoreference.

observed. Wave 3 is also found if the potential is scanned in a positive direction prior to scanning negative of wave 1. Cyclic voltammetric experiments were performed on $P(C_6H_5)_3$ under identical conditions, and wave 3 is not due to oxidation of free $P(C_6H_5)_3$. However, there is a shoulder on wave 3 (Figure 3a) at 1.33 V that is due to the presence of free $P(C_6H_5)_3$. When triphenyl phosphite is the added reactant, waves 1 and 2 are merged and occur at E_{pc} = −0.05 V and the value of E_{pa} for wave 3 is 1.76 V vs SCE (Figure 3b) at 100 mV/s. A strong shift in E_{pc} for wave 2 is not found under these conditions.

Wave 3 (Figure 3a) is due to oxidation of $Au[P(C_6H_5)_3]Cl$ as will be discussed in later sections of this text. Formation of $Au[P(C_6H_5)_3]Cl$ is implied under these conditions, and this is confirmed by UV–visible data. Upon addition of $P(C_6H_5)_3$ to $K[AuCl_4]$ dissolved in acetonitrile, TBAP, the absorption band at 321 nm for $K[AuCl_4]$ decreases to baseline and the final product observed has absorption bands at 272, 266, 259, and 225 nm. This is identical with that found for authentic samples of $Au[P(C_6H_5)_3]Cl$ in acetonitrile. Note that both $K[AuCl_4]$ and $Au[P(C_6H_5)_3]Cl$ have an absorption band at 225 nm.

Synthesis of $Au[P(R)_3]Cl$ by addition of $P(R)_3$ to $K[AuCl_4]$ has been reported,[4,25,26] and an interesting feature is that the rate of the chemical reaction is dependent upon the R group of $P(R)_3$. When R = C_6H_5, the reaction is complete within a few minutes, but when R = OC_6H_5, the reaction can take days at room temperature. If the reaction is chemically slow, we find that electrochemical reduction of $K[AuCl_4]$ in the presence of $P(R)_3$ is a convenient method to form and examine $Au[P(R)_3]Cl$. This

(30) Nicholson, R. S.; Shain, I. *Anal. Chem.* **1964**, *36*, 706.
(31) Mussini, T.; Faita, G. Chlorine. In *Encyclopedia of Electrochemistry of the Elements*; Bard, A. J., Ed.; Marcel Dekker: New York, 1973; Vol. 1, p 1.

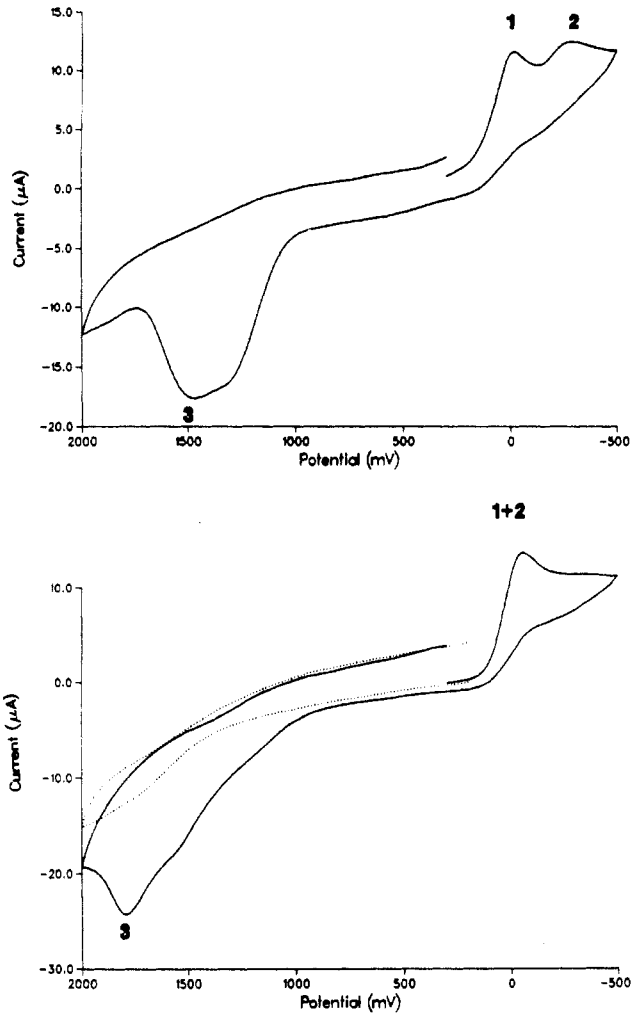

Figure 3. (a, Top) Cyclic voltammogram of a 0.0037 M solution of $K[AuCl_4]$ in acetonitrile, 0.237 M TBAP at 100 mV/s in the presence of 0.0045 M triphenylphosphine. (b, Bottom) Cyclic voltammogram of a 0.0045 M solution of $K[AuCl_4]$ in acetonitrile, 0.248 M TBAP at 100 mV/s in the presence of 0.0046 M triphenyl phosphite. The dotted line is the result if the potential is scanned in a positive direction from 0.30 V.

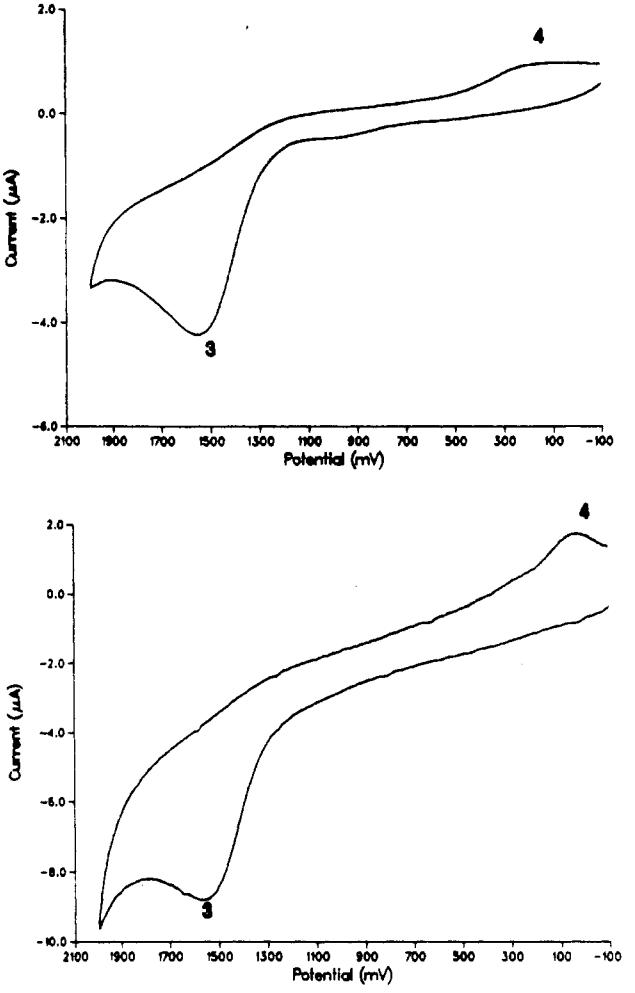

Figure 4. (a, Top) Cyclic voltammogram of a 0.0034 M solution of $Au[P(C_2H_5)_3]Cl$ in acetonitrile, 0.100 M TBAP. (b, Bottom) Cyclic voltammogram of a 0.0048 M solution of $Au[P(C_6H_5)_3]Cl$ in acetonitrile, 0.163 M TBAP.

is indicated in Figure 3b, in which a strong oxidation wave for $Au[P(OC_6H_5)_3]Cl$ is observed only after scanning negative of wave 1 and 2. Bulk electrolysis of $K[AuCl_4]$ at −0.20 V vs SCE in the presence of $P(OC_6H_5)_3$ gives values of n of 1.8 ± 0.1 with no evidence for formation of Au on the electrode surface.

On the basis of the reduction mechanism proposed for $[AuCl_4]^-$, $P(R)_3$ is most likely reacting with $[AuCl_2]^-$ following electrochemical reduction of $[AuCl_4]^-$, as shown in eq 4. This assignment

$$[AuCl_2]^- + P(R)_3 \rightleftharpoons Au[P(R)_3]Cl + Cl^- \qquad (4)$$

is supported by the observation that wave 2 strongly shifts to negative potentials in the presence of triphenylphosphine but not triphenyl phosphite, and hence the potential for wave 2 is sensitive to the kinetics of the added chemical reaction. It should be noted that this mechanism is valid in the presence of a reductive potential at an electrode surface. It cannot be directly applied to formation of $Au[P(R)_3]Cl$ from $P(R)_3$ and $AuCl_4^-$ in the absence of the electrode.

$Au[P(R)_3]Cl$, R = C_2H_5 and C_6H_5. Figure 4a shows the cyclic voltammogram of a 0.0034 M solution of $Au[P(C_2H_5)_3]Cl$ in acetonitrile, TBAP. This cyclic voltammogram is characterized by the presence of a broad oxidation wave (wave 3, Figure 4a) at E_{pa} = 1.51 V, which has a value of $E_{pa} - E_{pa/2}$ of 143 mV at a scan rate of 100 mV/s.

Process 3 is a diffusion-controlled process, since $i_p/v^{1/2}$ is constant and is irreversible in the sense that there is not a reduction process coupled to the oxidation. The value of E_{pa} shifts positively with an increase in scan rate, and these data suggest a process in which a chemical reaction follows electron transfer. Multiple scans indicate some filming of the electrode surface upon oxidation, requiring that the electrode surface be periodically cleaned. Bulk electrolysis experiments give a value of n of 2.0 ± 0.50. The large margin of error is due to the measurement of n with dilute solutions, to minimize the electrode filming effect.

The most distinctive feature of wave 3 is the value of $E_{pa} - E_{pa/2}$, which is much larger than that expected for a simple one- or two-electron transfer and can be explained by either slow electron-transfer kinetics or by an overlap of two electron-transfer processes coupled with chemical reaction(s), an ECE(C) process.[28] On the basis of cyclic voltammetric and the coulometric data, we assign the process at wave 3 as an ECE(C) process.

The other significant feature in Figure 4a is the presence of a small wave at E_{pc} of 0.20 V (wave 4, Figure 4a) at a scan rate of 100 mV/s. Wave 4 is observed only when the potential is scanned positive of wave 3, which means wave 4 is due to the reduction of a species formed by the oxidation of $Au[P(C_2H_5)_3]Cl$. Wave 4 is not well defined by cyclic voltammetry but is more pronounced in thin-layer cyclic voltammograms, since diffusion of any electrogenerated products away from the electrode is reduced. No reduction processes for $Au[P(C_2H_5)_3]Cl$ are observed out to −2.00 V vs SCE in acetonitrile.

The reduction of $[AuCl_4]^-$ in acetonitrile, 0.1 M TBAP gave waves at E_{pc} = 0.07 and −0.08 V at 100 mV/s (waves 1 and 2) and observation of wave 4 implies formation of a gold(III) ionic species, such as $[AuX_4]^-$, X = Cl^- and ClO_4^-. The shift in potential of wave 4 relative to waves 1 and 2 is due to an anion effect, since

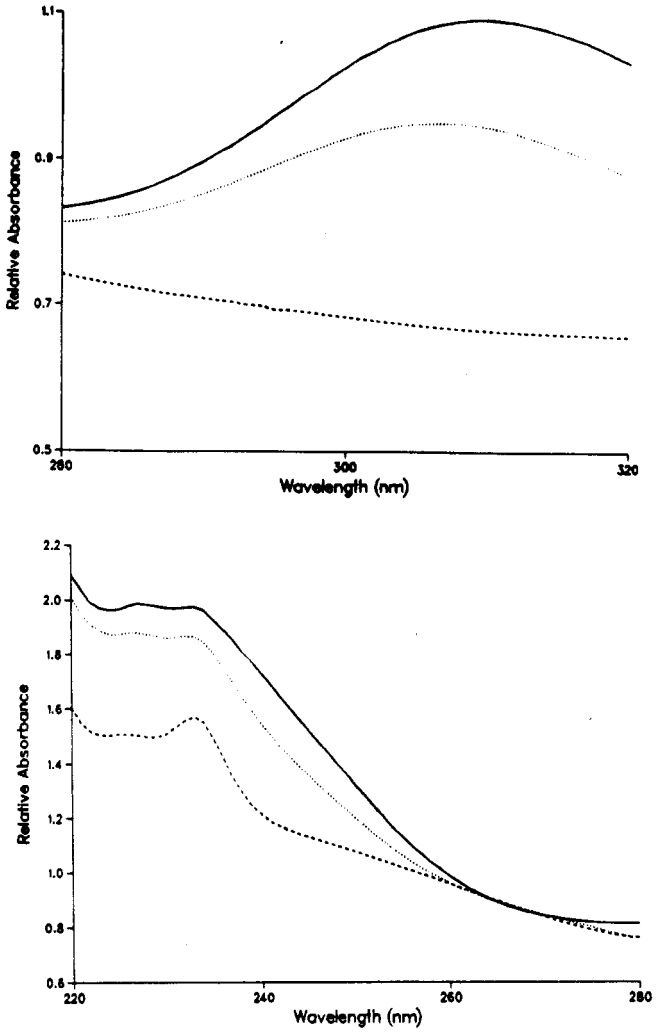

Figure 5. Spectroelectrochemical data for a 0.0067 M solution of Au[$P(C_2H_5)_3$]Cl in acetonitrile, 0.200 M TBAP: (a, top) spectral range 280–320 nm, E = 1.45 V; (b, bottom) spectral range 220–280 nm, E = 1.45 V. Key: original complex (---); T = 20 s (···); T = 2 min (—). Potentials are vs Pt a wire pseudoreference.

solutions of Au[$P(C_2H_5)_3$]Cl do not have sufficient chloride to form $[AuCl_4]^-$. The use of TBAP as the supporting electrolyte suggests formation of either $[Au(Cl)(ClO_4)_3]^-$ or $[Au(ClO_4)_4]^-$. However solvation by acetonitrile probably occurs, since perchlorate is a poor ligand.[32]

Similar electrochemical data were obtained for Au[$P(C_6H_5)_3$]Cl, and a representative cyclic voltammogram is shown in Figure 4b. In this case E_{pa} = 1.54 V for wave 3 in acetonitrile at 100 mV/s, while wave 4 is observed at an E_{pc} of 0.03 V.

It is important to note that the oxidation processes in Figure 4b and in Figure 3a are the same, which further demonstrates generation of Au[$P(C_6H_5)_3$]Cl from $K[AuCl_4]$ and $P(C_6H_5)_3$. Hence, generation of Au[$P(R)_3$]Cl by addition of $P(R)_3$ to $K[AuCl_4]$ provides a convenient technique to measure basic electrochemical properties of Au[$P(R)_3$]Cl complexes. Electrochemical data for Au[$P(R)_3$]Cl with R = OC_2H_5 and OC_6H_5 were obtained by this method. In general, these data are nearly the same as those found for Au[$P(C_2H_5)_3$]Cl and are summarized in Table I. The significant difference is the value of the potential for the oxidation of Au[$P(R)_3$]Cl (wave 3).

As seen in Table I, the value of E_{pa} for Au[$P(R)_3$]Cl is dependent on the ligand $P(R)_3$. As R changes from C_2H_5 and C_6H_5 to OC_2H_5 and OC_6H_5, the oxidation potential becomes more positive. This is in agreement with a decrease in the electron-donating power of the ligand. No significant change is found for the different phosphite or phosphine ligands; i.e., wave 3 is at the same potential when $P(R)_3$ is $P(C_6H_5)_3$ and $P(C_2H_5)_3$. Table I also demonstrates that there is a 0.22-V shift positive in the oxidation potential of Au[$P(C_2H_5)_3$]Cl when the solvent is changed from CH_3CN to CH_2Cl_2. A similar shift of 0.13 V is found when $P(R)_3$ is C_6H_5. When THF is the solvent, wave 3 for the gold trialkylphosphine complexes is near the solvent limit and an accurate reading is not possible. This solvent effect can be rationalized by either a stabilization of the oxidation product, $[AuX_4]^-$, in acetonitrile or by solvent coordination to Au[$P(R)_3$]Cl.

Figure 5 shows the spectroelectrochemical data obtained for the oxidation of a 0.0067 M solution of Au[$P(C_2H_5)_3$]Cl in acetonitrile, TBAP. The initial complex has no bands in the region of 320–280 nm,[25,26] but upon oxidation a band is formed at 310 nm. This is shown in Figure 5a. This band is assigned to $[AuX_4]^-$ in acetonitrile and is shifted by 11 nm relative to that for $[AuCl_4]^-$. This shift is assigned to the change in anions.

Reduction of the oxidized solution only at potentials negative of wave 4 cause the band at 310 nm to decrease to the baseline This is consistent with wave 4 of Figure 3a, corresponding to reduction of the product generated upon oxidation of Au[$P(C_2H_5)_3$]Cl.

The complex Au[$P(C_2H_5)_3$]Cl has a ligand absorption band at 233 nm,[25,26] which does not shift upon oxidation, as shown Figure 5b. Au[$P(C_2H_5)_3$]Cl also has a weak absorption band at 225 nm, which increases in intensity and shifts to 227 nm upon oxidation. This is due to formation of a new band at 227 nm (Figure 5b), which is also assigned to $[AuX_4]^-$. Reduction of the oxidized solution at potentials negative of wave 4 results in formation of the original spectrum and demonstrates generation of Au[$P(C_2H_5)_3$]Cl upon reduction of the oxidized solution.

The spectroelectrochemical results for Au[$P(C_6H_5)_3$]Cl parallel that found for Au[$P(C_2H_5)_3$]Cl and suggest that formation of $[AuX_4]^-$ upon oxidation of Au[$P(R)_3$]Cl is a general process. In addition, formation of Au[$P(C_6H_5)_3$]Cl occurs upon reduction of the oxidized solutions. Table II provides a summary of the spectroelectrochemical data for the different complexes.

Addition of $P(R)_3$ to Au[$P(R)_3$]Cl. The reaction of $P(R)_3$ with Au[$P(R)_3$]Cl has been studied, and the species $Au[P(R)_3]_n^+$, n = 2–4, have been reported,[4,33–35] as shown in eq 5. The principal

$$Au[P(R)_3]Cl + P(R)_3 \rightleftharpoons Au[P(R)_3]_n^+ + Cl^- \quad n = 2\text{–}4 \tag{5}$$

species present depends upon the concentration of $P(R)_3$ and the size of the R group. When R = C_6H_5, the primary species in solution are Au[$P(R)_3$]Cl and $Au[P(R)_3]_2^+$, on the basis of IR and conductivity results.[33] However, the n = 3 and 4 species have been reported.[35]

This reaction was monitored electrochemically and resulted in data on the bis species, $Au[P(C_6H_5)_3]_2^+$. In our experiments, the concentration of the added $P(C_6H_5)_3$ was kept low, so the principal

Table II. Spectroelectrochemical Data for the Studied Complexes (Acetonitrile, TBAP)

complex		λ_{max}, nm			
$K[AuCl_4]$	no potential	225	321		
	E = –0.7 V[a]	no abs bands			
Au[$P(C_2H_5)_3$]Cl	no potential	225	233		
	E = 1.45 V[a]	227	233	310	
Au[$P(C_6H_5)_3$]Cl[b]	no potential	260	266	274	
	E = 1.90 V[a]	260	266	274	309[c]

[a] Potential applied to working electrode, vs Pt wire pseudoreference. [b] Spectral range 250–350 nm. [c] Broad absorption found in this region.

(32) It has been suggested by a reviewer that the species $(Au[P(R)_3]ClS_2)^{2+}$, where S is solvent, is formed rather than AuX_4^-.

(33) Jones, P. G.; Sheldrick, G. M.; Muir, J. A.; Pulgar, L. B. *J. Chem. Soc., Dalton Trans.* **1982**, 2123.
(34) Meyer, J. M.; Allred, A. L. *J. Inorg. Nucl. Chem.* **1968**, *30*, 1328.
(35) Jones, P. G.; Sheldrick, G. M.; Muir, M. M.; Pulgar, L. B. *J. Chem. Soc., Dalton Trans.* **1979**, 1112.

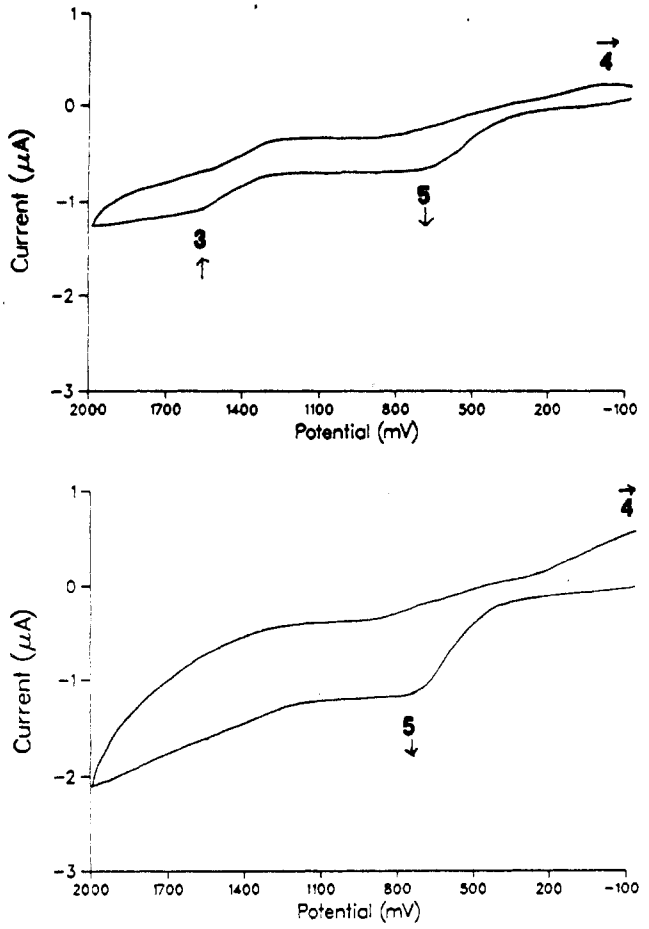

Figure 6. Cyclic voltammogram of a 0.0048 M solution of $Au[P(C_6H_5)_3]Cl$ in acetonitrile, 0.16 M TBAP in the presence of (a, top) 0.0032 M and (b, bottom) 0.0059 M $P(C_6H_5)_3$.

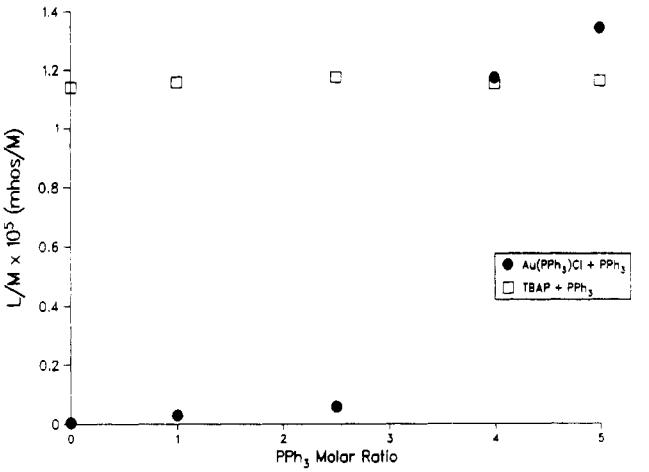

Figure 7. Molar conductivity of a 0.0027 M solution of $Au[P(C_6H_5)_3]Cl$ (●) and 0.0055 M solution of TBAP (□) in acetonitrile as a function of added $P(C_6H_5)_3$.

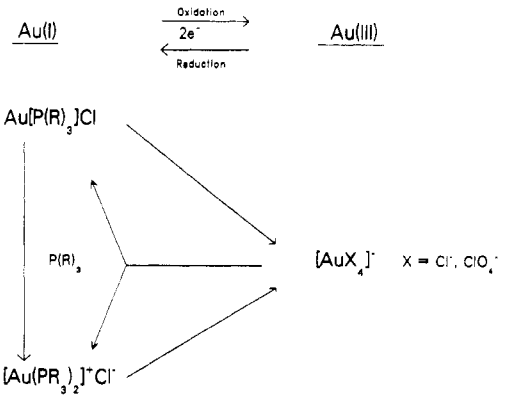

Figure 8. Electron-transfer scheme for $K[AuCl_4]$, $Au[P(R)_3]Cl$, and $Au[P(R)_3]_2^+$.

species present are $Au[P(R)_3]Cl$ and $Au[P(R)_3]_2^+$.

An example of the electrochemical data obtained for this reaction is shown in Figure 6. Figure 6a shows the cyclic voltammogram obtained when 1.2 equiv of $P(C_6H_5)_3$ is added to a 0.0048 M solution of $Au[P(C_6H_5)_3]Cl$ in 0.16 M TBAP, CH_3CN. Under these conditions, wave 3 shifts to E_{pa} = 1.60 V at 100 mV/s and decreases in current and a new electron-transfer process at E_{pa} = 0.77 V is observed (wave 5, Figure 6a). The fact that wave 3 shifts to positive potentials upon addition of $P(C_6H_5)_3$ supports loss of $P(R)_3$ upon oxidation of $Au[P(R)_3]Cl$. Note that wave 4, or the reduction of electrogenerated $[AuX_4]^-$, is still observed. Wave 3 continues to decrease while wave 5 continues to increase as more $P(C_6H_5)_3$ is added. At 2.3 equiv of $P(C_6H_5)_3$, wave 5 is the predominant electron-transfer process and wave 4 is still present but has shifted in a negative direction, as shown in Figure 6b. This is similar to the shift found for the reduction of $K[AuCl_4]$ upon addition of $P(C_6H_5)_3$. It should be noted that $P(C_6H_5)_3$ was examined under identical conditions and is not the cause of wave 5 but does account for the increase in the background above 1.10 V.

Conductivity data were obtained for the titration of $P(C_6H_5)_3$ to $Au[P(C_6H_5)_3]Cl$ in acetonitrile, with TBAP as the standard. Upon addition of $P(C_6H_5)_3$ to $Au[P(C_6H_5)_3]Cl$, the solution changed from a nonelectrolyte to a 1:1 electrolyte. As expected, addition of $P(C_6H_5)_3$ to the reference solution (TBAP) had little effect. These data are presented in Figure 7 and are consistent with earlier conductivity data reported for this system.[27] Hence, wave 5 is observed upon formation of $Au[P(C_6H_5)_3]_2^+$ and is assigned to the oxidation of this species.

The potential for the oxidation of $Au[P(C_6H_5)_3]_2^+$ is strongly shifted negative relative to $Au[P(C_6H_5)_3]Cl$. This is somewhat surprising given that the oxidation of the positively charged species is significantly easier than that of the related neutral complex. The exact reason for the shift is not known but indicates a large stabilization by Cl^- of the gold(I) state.

For wave 5, a coupled reduction process is not found and E_{pa} shifts in a positive direction with scan rate. In addition, $E_p - E_{p/2}$ is again large, 190 mV at a scan rate of 100 mV/s and $i_p/v^{1/2}$ is constant. A dependence of E_{pa} on the concentration of $P(R)_3$ is also found that suggests ligand loss upon oxidation. This is in agreement with the fact that wave 4, or the reduction of the electrogenerated $[AuX_4]^-$, is still observed. These data imply that oxidation of $Au[P(C_6H_5)_3]_2^+$ also results in formation of $[AuX_4]^-$.

Similar to experiments in which generation of $Au[P(R)_3]Cl$ is observed electrochemically, monitoring the formation of $Au[P(R)_3]_2^+$ from solutions of $K[AuCl_4]$ and $P(R)_3$ is also possible. For example, if additional amounts of $P(C_6H_5)_3$ are added to the system described in Figure 3a, wave 5 is again observed. This is expected and is consistent with the reaction properties of $Au[P(C_6H_5)_3]Cl$. Hence, by in situ generation of $Au[P(OC_2H_5)_3]_2^+$ electrochemical data (E_{pa}) for the oxidation of this species were obtained. However, under these conditions, significantly greater amounts of $P(R)_3$ are necessary to observe the bis species (wave 5) by the cyclic voltammetric experiment. Similar to $Au[P(R)_3]Cl$, as R is changed from a trialkylphosphine to a trialkyl phosphite, the oxidation potential shifts in a positive direction.

Figure 8 shows the electron-transfer mechanism for the gold complexes that have been studied. The species $[AuX_4]^-$ and $Au[P(R)_3]Cl$ can be generated from one another by redox processes with addition or loss of $P(R)_3$. A similar relationship between $[AuX_4]^-$ and $Au[P(R)_3]_2^+$ is indicated. The formation of $Au[P(R)_3]_2^+$ by addition of $P(R)_3$ to solutions of $Au[P(R)_3]Cl$ is also presented.

As shown in this study, the nature of the ligands coordinated to gold(I) species have a significant influence on the electro-

chemical properties. The positive shift in potential upon formation of $Au[P(R)_3]_2^+$ may have important biological implications. For example, formation of $Au[P(C_2H_5)_3](SR)^+$ where SR is a sulfur-containing ligand such as cysteine-34 of mercaptalbumin occurs[7,8] when either $Au[P(C_2H_5)_3]Cl$ or $Au[P(C_2H_5)_3]_2^+$ is added to a matrix modeling biological systems. If the potential for the oxidation of $Au[P(C_2H_5)_3](SR)^+$ is also significantly shifted to lower potentials, this species could become active toward redox reactions.

Acknowledgment. Partial support from a Boston College annual research grant is gratefully acknowledged.

Contribution from the Department of Chemistry, and the LASER Laboratory, Michigan State University, East Lansing, Michigan 48824, and Laboratory of Biochemistry, University of Amsterdam, P.O. Box 20151, 1000 HD Amsterdam, The Netherlands

Factors Affecting the Iron–Oxygen Vibrations of Ferrous Oxy and Ferryl Oxo Heme Proteins and Model Compounds

W. Anthony Oertling,[†,§] Robert T. Kean,[†,∥] Ron Wever,[‡] and Gerald T. Babcock*[,†]

Received August 29, 1989

Resonance Raman (RR) and UV–visible absorption spectra of various imidazole-ligated ferrous oxy ($Fe^{II}—O_2$) and ferryl oxo ($Fe^{IV}=O$) porphyrins are presented. Because physiologically relevant porphyrins have been used in this study, these measurements provide a basis to identify protein-induced changes in the iron–oxygen vibrations, as well as in the structure-sensitive macrocycle vibrations and in the optical absorption spectra, of heme enzyme intermediates. The iron–oxygen stretching frequencies, $\nu(Fe^{IV}=O)$, of ferryl oxo complexes of octaethylporphyrin (OEP), protoporphyrin IX dimethyl ester (PPDME), and tetraphenylporphyrin (TPP) in toluene at −120 °C reported here, together with results from other model compounds, are used to interpret the values of $\nu(Fe^{IV}=O)$ reported for ferryl-oxo myoglobin and the catalytic intermediates of several peroxidase enzymes. We identify the major protein influence on the $\nu(Fe^{IV}=O)$ frequency to be the trans-ligand strength of the proximal histidine, with a minor, but nonetheless important, effect being imposed by distal hydrogen bonding of the oxo ligand (Sitter, A. J.; Reczek, C. M.; Terner, J. *J. Biol Chem.* **1985**, *260*, 7515–7522. Hashimoto, S.; Tatsuno, Y.; Kitagawa, T. *Proc. Natl. Acad. Sci. U.S.A.* **1986**, *83*, 2417–2421). This analysis follows from the inverse correlation we identify for $\nu(Fe^{IV}=O)$ with respect to $\nu(Fe^{II}=His)$. For the ferrous oxy complexes of OEP, protoporphyrin IX (PP), and porphyrin *a* (PA) in DMF and CH_2Cl_2 at −120 °C, the $\nu(Fe^{II}=O_2)$ values we obtain are compared with similar measurements on other model compounds. As opposed to the ferryl oxo systems, in which $\nu(Fe^{IV}=O)$ correlates inversely with trans-ligand strength, a direct correlation exists between $\nu(Fe^{II}=O_2)$ and the strength of the iron/trans-ligand interaction in the model systems (Walters, M. A.; Spiro, T. G.; Suslick, K. S.; Collman, J. P. *J. Am. Chem. Soc.* **1980**, *102*, 6857–6858. Kerr, E. A.; Mackin, H. C.; Yu, N.-T. *Biochemistry* **1983**, *22*, 4373–4379). Moreover, we interpret the available data to indicate that $\nu(Fe^{II}—O_2)$ correlates inversely with $\nu(O=O)$ of bound dioxygen. We use these observations to evaluate the iron–oxygen vibrations of oxy myoglobin, horseradish peroxidase compound III, and an early intermediate in the reduction of O_2 by cytochrome *c* oxidase; we conclude that the iron–oxygen stretching frequencies displayed by the various ferrous oxy proteins can be understood in terms of distal influences on the electron density in the O=O bond.

Introduction

Two intermediates of considerable interest in reactions catalyzed by heme proteins are ferrous oxy ($Fe^{II}—O_2$) and ferryl oxo ($Fe^{IV}=O$) compounds. The ferrous oxy species is exemplified by hemoglobin and myoglobin, which bind O_2 reversibly when the heme is in a ferrous state. The initial intermediate in the reduction of dioxygen by cytochrome *c* oxidase[1] is a ferrous oxy compound,[2,3] and a ferrous oxy species has been identified as a reaction intermediate of cytochrome P-450.[4] Dioxygen binding can also be easily induced in ferrous peroxidase samples to produce a ferrous oxy species (compound III), which can, alternatively, be formed by the addition of excess H_2O_2 to the ferric enzyme.[5] Ferryl oxo species have been postulated in the catalytic cycle of cytochrome *c* oxidase,[6] as the oxygen-donating species in cytochrome P-450,[7] and as intermediates in the reactions of catalases and peroxidases.[8] Addition of peroxide to the normally unreactive globin hemes can also induce the formation of ferryl species.[9] The variation in reactivity and catalytic function of both ferrous oxy and ferryl oxo species in different proteins suggests protein variations in the heme vicinity. Identification of these protein differences should provide considerable insight into the catalytic mechanisms of these proteins.

Resonance Raman spectroscopy (RR) has the resolution necessary to probe these protein-specific structural variations and has been applied to ferrous oxy heme proteins.[10-15] Recently Varotsis et al.[3] have used two-color, time-resolved RR measurements of

† Michigan State Unversity.
‡ University of Amsterdam.
§ Present address: INC-4, Mail Stop C-345, Los Alamos National Laboratory, Los Alamos, NM 87545.
∥ Present address: Cargill Inc., Research Division, P.O. Box 9300, Minneapolis, MN 55440.

(1) (a) Wikstrom, M.; Krab, K.; Saraste, M. *Cytochrome Oxidase, A Synthesis*; Academic Press: New York, 1981. (b) Naqui, A.; Chance, B. *Annu. Rev. Biochem.* **1986**, *55*, 137–166. (c) Hill, B. C.; Greenwood, C.; Nicholls, P. *Biochim. Biophys. Acta* **1986**, *853*, 91–113. (d) Chan, S. I.; Witt, S. N.; Blair, D. F. *Chem. Scr.* **1988**, *28A*, 51–58. (e) Babcock, G. T. In *Biological Applications of Raman Spectroscopy*; Spiro, T. G., Ed.; Wiley: New York, 1988; pp 293–346.
(2) (a) Babcock, G. T.; Jean, J. M.; Johnston, L. N.; Palmer, G.; Woodruff, W. H. *J. Am. Chem. Soc.* **1984**, *106*, 8305–8306. (b) Babcock, G. T.; Jean, J. M.; Johnston, L. N.; Woodruff, W. H.; Palmer, G. *J. Inorg. Biochem.* **1985**, *23*, 243–251.
(3) (a) Varotsis, C.; Woodruff, W. H.; Babcock, G. T. *J. Am. Chem. Soc.* **1989**, *111*, 6439–6440; *J. Am. Chem. Soc.* **1990**, *112*, 1297. (b) Varotsis, C.; Woodruff, W. H.; Babcock, G. T. *J. Biol. Chem.*, in press.
(4) (a) Peterson, J. A. *Biochem. Biophys. Res. Commun.* **1971**, *42*, 140–142. (b) Bangcharoenpaurpong, O.; Rizos, A.; Champion, P. M.; Jollie, D.; Sligar, S. *J. Biol. Chem.* **1986**, *261*, 8089–8092.
(5) (a) Keilin, D.; Mann, T. *Proc. R. Soc. London, B* **1937**, *122*, 119–133. (b) Wittenberg, J. B.; Noble, R. W.; Wittenberg, B. A.; Antonini, E.; Brunori, M.; Wyman, J. *J. Biol. Chem.* **1967**, *242*, 626–634. (c) Nakajima, Ryo; Yamazaki, I. *J. Biol. Chem.* **1987**, *262*, 2576–2581.
(6) (a) Wikstrom, M. *Proc. Natl. Acad. Sci. U.S.A.* **1981**, *78*, 4051–4054. (b) Blair, D. F.; Witt, S. N.; Chan, S. I. *J. Am. Chem. Soc.* **1985**, *107*, 7389–7399.
(7) Groves, J. T. In *Cytochrome P-450: Structure, Mechanism and Biochemistry*; Ortiz de Montellano, P., Ed.; Plenum Press: New York, 1986; Chapter 1.
(8) (a) Dunford, H. B. *Adv. Inorg. Biochem.* **1982**, *4*, 41–68. (b) Few, J. E.; Jones, P. In *Advances in Inorganic and Bioinorganic Mechanism*; Academic Press: New York, 1984; Vol. 3, pp 175–212.
(9) (a) George, P.; Irvine, D. H. *Biochem. J.* **1952**, *52*, 511–517. (b) Uyeda, M.; Peisach, J. *Biochemistry* **1981**, *20*, 2028–2035.
(10) Brunner, H. *Naturwissenschaften* **1974**, *61*, 129.
(11) Duff, L. L.; Applemen, E. H.; Shriner, D. F.; Klotz, I. M. *Biochem. Biophys. Res. Commun.* **1979**, *90*, 1098–1103.

0020-1669/90/1329-2633$02.50/0